ELSEVIER

Catalysis Today 42 (1998) 61–71

CATALYSIS TODAY

# Lean-$NO_x$ reduction catalysis by metal-complex impregnated molecular sieves – Effect of ligands and metals

Partha P. Paul*, Martin J. Heimrich, Michael A. Miller

*Southwest Research Institute, 6220 Culebra Road, San Antonio, TX 78238, USA*

## Abstract

We have developed lean-$NO_x$ catalysts using modified mesoporous molecular sieves which operate under very low hydrocarbon concentrations. Transition metal (copper and iron)-complex impregnated mesoporous molecular sieves have been synthesized. Cryptand type ligands (L1 and L2) have been used for complex formation. The ligand plays a crucial role in the complex formation and catalytic activity. These metal-complex impregnated molecular sieves are further treated with $[Pd(NH_3)_4]\,Cl_2$. Fe–L2 and Cu–L2-based catalysts are active towards $NO_x$ reduction under oxygen rich (lean-$NO_x$) conditions. The catalytic activity towards $NO_x$, CO and HC was studied using simulated exhaust gas, as well as engine exhaust gas from a lean burning gasoline engine. Using engine exhaust gas at an air/fuel ratio of 16.10, test results showed a reduction of $NO_x$ up to 10% at inlet temperatures ranging from 260°C to 285°C and $HC/NO_x=2/1$.

*Keywords:* Lean-$NO_x$; Mesoporous molecular sieves; Metal-complex impregnation; Emission control; $NO_x$ reduction

## 1. Introduction

Atmospheric $NO_x$, which primarily consists of NO and $NO_2$, results in air pollution and the production of acid rain. $NO_2$ has been linked to bronchitis, pneumonia and alteration of the immune system. It is also responsible for acid rain and urban smog. $NO_x$ also participates in the formation of ground-level ozone in the presence of sunlight. Industrial and other combustion processes (e.g. automobiles) produce large amounts of $NO_x$, which is a severe threat to the environment.

About one-half of all man-made emissions of $NO_x$ can be attributed to automobile engine emissions [2]. The 1990 Clean Air Act (USA) restricts automobile engine emissions. In addition, there is a considerable interest between automobile manufacturers and regulators to increase vehicle fuel economy. One of the possible ways of reducing the emissions and increasing fuel economy is through the use of lean-burn engines, such as diesel engines and lean-burn gasoline or natural gas engines. These engines operate at leaner fuel-to-air ratios than that required for stoichiometric combustion of fuel. A conventional three-way catalyst (TWC) fails to provide $NO_x$ reduction under lean-burn (oxygen-rich) conditions. Lean-$NO_x$ catalysis is inherently a difficult process because of two competing reactions (Eqs. (1) and (2)). The hydrocarbon needed as a reductant for the conversion of $NO_x$ gets oxidized by oxygen under catalytic conditions:

$$NO_x + (CH_2)_n + O_2 \rightarrow N_2 + nCO_2 + nH_2O \qquad (1)$$

$$(CH_2)_n + O_2 \rightarrow nCO_2 + nH_2O \qquad (2)$$

---

*Corresponding author.

0920-5861/98/$32.00
*PII* S0920-5861(98)00077-7

Metal ion exchanged zeolites have been investigated as lean-$NO_x$ catalysts [1]. Some of these catalysts are active only under a huge excess of supplemental hydrocarbons. However, it defeats the fuel-efficiency benefits obtained by lean-burn engines. While catalytic $NO_x$ reduction under oxygen-rich conditions poses chemical and engineering problems, natural enzymes, such as nitric oxide reductase [3] and nitrous oxide reductase [4], reduce nitrogen oxides with ease. The active sites of $NO_x$ reducing enzymes contain multinuclear iron or copper ions ligated by nitrogen, oxygen and sulfur donor atoms which are supported in the protein [3]. A chemical system capable of mimicking such an enzyme [5] might selectively reduce $NO_x$ in the presence of oxygen. A metal–ligand complex imbedded in an inorganic polymer, such as a zeolite/molecular sieve, can serve as a biomimetic model for $NO_x$ reduction. Using a biomimetic approach, we have reported [6] our preliminary finding of $NO_x$ catalysis by iron complex impregnated mesoporous molecular sieves such as MCM-41. Here we report a more complete study which includes the catalytic activity of copper complex impregnated molecular sieves. For this study, we have used nitrogen containing cryptand ligands L1 and L2 which are shown in Fig. 1. By carefully choosing the ligand, the redox potential of the metal complex can be adjusted so that preferential reduction of $NO_x$ is carried out, even under an excess of oxygen. Effects of ligand and the metal ion on the catalytic activity is presented in this paper.

## 2. Experimental

### 2.1. Materials and equipment

All synthetic manipulations were carried out under dry nitrogen or argon using standard schlenk techniques [7]. $FeSO_4 \cdot 7H_2O$ was obtained from Fisher Scientific. $[Cu(CH_3CN)_4]$ $[PF_6]$, terephthalaldehyde, and *tris*(2-aminoethyl)amine (TREN) were obtained from Aldrich, and were used as received. 2,6 diacetyl pyridine was obtained from Fluka. $Pd(NH_3)_4Cl_2$ was obtained from Pfaltz&Bauer. Amorphous silica, Ultrasyl, was obtained from PQ Corporation. Sodium aluminate was obtained from United Mineral and Chemical Corporation. Cetyltrimethylammonium bromide was obtained from Zeeland Chemicals. $CH_3CN$ and DMF were distilled from $CaH_2$ and barium oxide, respectively. The autoclave and its controller used for the molecular sieves synthesis were obtained from Parr Instruments. Fourier transformed infrared (FTIR) spectra were obtained on a Bio-Rad Digilab Model FTS-15E/D FTIR spectrometer equipped with a Bio-Rad Digilab 3240 data system. Powder X-ray diffraction analyses were conducted with a Siemens D-500 X-ray diffractometer. A Lambda Array 3840 UV–vis spectrophotometer was used for diffused reflectance spectra. A thermal desorption and recoiling mass spectrometer (TDARMS) system, developed at Southwest Research Institute (SwRI), was employed to determine the efficacy of catalyst materials. The exhaust emission tests were performed in the emission laboratories at SwRI.

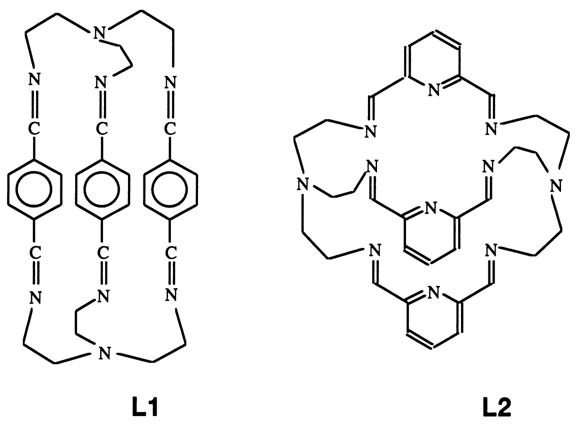

Fig. 1. Cryptand ligands used to synthesize Cu(I) and Fe(II) impregnated molecular sieves.

### 2.2. Synthesis of ion exchanged mesoporous molecular sieves

*Preparation of mesoporous molecular sieve*. The mesoporous molecular sieves were synthesized by making minor variations to the reported method [8]. A solution of cetyltrimethylammonium bromide (41 g) in 100 ml of deionized water was added to 65 g of Ultrasil. A 50 ml deionized water solution containing 3 g of sodium aluminate, and a 50 ml deionized $H_2O$ solution of 21 g NaOH were also added. The mixture was diluted with 200 ml of deionized water. The mixture was poured in an autoclave, and stirred at 150°C for 10 h. It was stored at 150°C for another 12 h without stirring. The solid formed was washed repeatedly with water, dried in air for 18 h, and calcinated at 540°C.

Fe(II) *exchange of the mesoporous molecular sieve*. The ion exchanges were conducted using a procedure very similar to the reported method [9]. A solution of nearly 2 g $Fe(II)SO_4$ in ~550 ml of water was added to mesoporous molecular sieves (MCM-41) (~10 g) and refluxed under nitrogen. The ion exchanged molecular sieves were washed several times with hot water and dried under vacuum at 150°C.

Cu(I) *exchange of the mesoporous molecular sieves*. 2 g of $[Cu(CH_3CN)_4]\ PF_6$ was dissolved in 100 ml of dry acetonitrile. To that solution, 10 g of mesoporous molecular sieves (MCM-41) were added and the mixture was refluxed overnight. The ion exchanged sieves were washed thoroughly with acetonitrile and dried in vacuum at 100°C.

### 2.3. Synthesis of metal-complex impregnated large pore molecular sieves

Cu(I)–L1 *complex inside the molecular sieve pore*. To a solution of TREN (1.0 ml, 6.72 mmol) in 25 ml of acetonitrile, a 25 ml solution of terephthalaldehyde (1.3 g, 9.70 mmol) was added dropwise over a period of an hour. After stirring for 15 min, the solution was cloudy, indicating the formation of L1. At this time, 5 g of Cu(I) exchanged molecular sieve was added. The colorless molecular sieve became bright yellow in 10 min. The mixture was further stirred for 16 h, and then washed with $CH_3CN$ several times. After soxhlet extraction with $CH_3CN$ for 2–3 days, the solid was dried under vacuum.

Fe(II)–L1 *complex inside the molecular sieve pore*. A procedure similar to that in the case of the Cu(I)–L1 was used; however, no reaction was observed.

Fe(II)–L2 *complex inside the molecular sieve pore*. To a solution of TREN (0.7 ml, 4.70 mmol) in 25 ml of acetonitrile, a 25 ml solution of 2,6 diacetyl pyridine (1.14 g, 6.99 mmol) in acetonitrile was added dropwise over a period of 1 h. A pale yellow solution of L2 resulted, to which 5 g of Fe(II) exchanged molecular sieve was added. The molecular sieve became dark-blue in 20 min, which was further stirred for 16 h. The mixture was washed several times with $CH_3CN$, followed by soxhlet extraction for several days. The solid was then dried under vacuum.

Cu(I)–L2 *complex inside the molecular sieve pore*. A procedure similar to that used for Fe(II)–L2 impregnation was employed. Reacting a colorless Cu(I) exchanged molecular sieve with a solution of L2, an air-sensitive brick-red solid resulted. After washing the solid several times with acetonitrile, soxhlet extraction was carried out with acetonitrile. The solid was dried under vacuum.

### 2.4. Palladium incorporation and preparation of the catalysts

The molecular sieves with impregnated metal complexes were further treated with Pd(II) ions. In general, a solution of $[Pd(NH_3)_4]Cl_2$ in DMF was added to the impregnated molecular sieves and the mixtures were stirred at 70°C for 16 h. The solids were filtered and washed with DMF. Soxhlet extraction of the soluble impurities with acetonitrile and drying under vacuum produced the desired catalysts. Cu(I)–L1, Cu(I)–L2 and Fe(II)–L2 impregnated complexes when treated with $[Pd(NH_3)_4]Cl_2$ resulted in golden-yellow, red-brown and black-blue colored solids, respectively, which are designated as catalysts A, B and C.

### 2.5. Catalytic activity with simulated exhaust gas

A thermal desorption and recoiling mass spectrometer (TDARMS) system was employed to determine the efficacy of catalysts A, B and C. This system, designed and constructed specifically for studies of catalyst/substrate gas-phase processes, consists of a process chamber, containing a heating stage and a test-material quartz crucible, that is interfaced to a

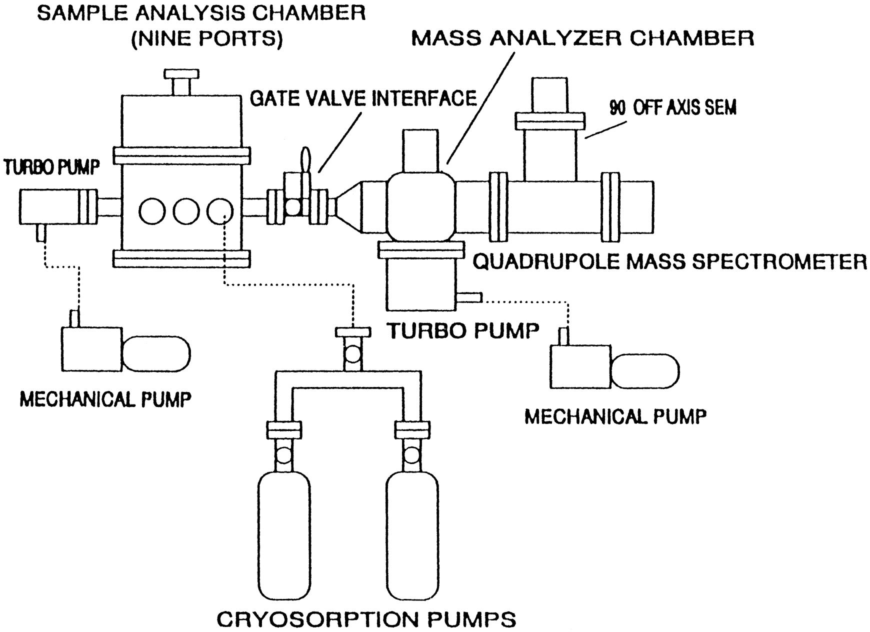

Fig. 2. A sketch of SwRI developed thermal desorption and recoiling mass spectrometer (TDARMS).

quadruple mass spectrometer (QMS) and a piezoelectric leak valve for gas introduction. High vacuum in the process chamber and in the QMS is achieved through turbomolecular pumps and cryosorption pumps, thus ensuring extremely low background contamination. A sketch of the TDARMS system is shown in Fig. 2.

Finely powdered catalysts A, B, and C (1 g) were weighed directly into a quartz crucible. A thin layer of quartz wool was then placed over the powder to prevent the material from becoming dispersed in the process chamber during initial evacuation. After placing the crucible containing the catalyst in the process chamber, the chamber was evacuated to approximately $10^{-3}$ Torr using the cryosorption pumps. Ultimate vacuum ($10^{-7}$ Torr) was then achieved by using the turbomolecular pump and allowing the chamber to equilibrate for a period of at least 24 h. Thermal equilibrium was also achieved during this period at the desired temperature.

Background spectra were taken at two different temperatures (100°C and 200°C). The reactive process was carried-out at a steady-state leak of the source gas (2% $^{15}$NO and 2% $^{13}$CO with a balance of argon+2% $H_2O$ and 2% $O_2$ in balance He) by applying a gradient voltage to the piezoelectric leak valve until a constant total pressure of 1.5–5 Torr was achieved as measured at the QMS. The source gas was allowed to interact with the catalyst material at this constant pressure while multiple analog scans were monitored and digitally recorded for later manipulation.

### 2.6. *Catalytic activity with engine exhaust gas*

Catalysts B and C were tested for $NO_x$, HC, and CO activity with engine exhaust produced under lean-burn conditions.

*Preparation of the sample.* Catalysts B and C were coated on cylindrical 2.54 cm dia.×2.54 cm length (1 inch dia.×1 inch length) cordierite substrates with square cell geometry containing 400 cells per square inch. The catalysts were stirred with acetonitrile to obtain a slurry. The cordierite substrates were dipped in the slurry and dried under a flow of nitrogen. This process was repeated three times. The substrates were then heated to 100°C under nitrogen. The dipping and drying steps were repeated three more times so that the catalyst loading was nearly 2 g per cubic inch (0.12 g $cm^{-3}$) of the cordierite support. The catalyst was finally heated to 100°C for 2 h.

Table 1
Engine exhaust gas composition

| Emission | Concentration |
|---|---|
| Hydrocarbons | 825 ppmC (without supplemental HC)<br>4000 ppmC (with supplemental HC) |
| Carbon monoxide (CO) | 4000 ppm |
| Oxides of nitrogen ($NO_x$) | 2000 ppm |
| Oxygen ($O_2$) | 3.0% |

Concentrations of hydrocarbons measured as $C_1$

*Test procedure*. Catalysts B and C were tested under lean (oxygen-rich relative to stoichiometry) conditions on a 350 cubic inch displacement (CID) gasoline engine manufactured by Chevrolet. Air was added to the exhaust gas to increase the oxygen content to 3%. Consequently, the air–fuel (exhaust gas) ratio was 16.10. The CO concentration was twice that of the $NO_x$ concentration, as shown in Table 1. Different hydrocarbon (HC) concentrations (825 and 4000 ppmC) were used in the evaluation of catalyst C. High concentrations of HC were achieved with supplemental hydrocarbons added to the exhaust. Gasoline was injected into the exhaust gas to provide hydrocarbon enrichment to approximately 4000 ppmC. Catalyst inlet HC-to-$NO_x$ (HC/$NO_x$) ratios with HC enrichment were approximately 2.0/1.0. Without supplemental hydrocarbons added to the exhaust, catalyst inlet HC-to-$NO_x$ ratios were approximately 0.42/1.0. Catalyst light-off tests were performed by simultaneously measuring the concentration of HC, CO, and $NO_x$ in the exhaust gas upstream and downstream of the catalysts over a specified temperature range. Each catalyst light-off test was performed as a series of discrete steady-state conditions and sequentially performed starting at low temperatures and proceeding to higher temperatures.

Exhaust gas delivered to the catalyst was maintained at the desired temperature using a water-cooled heat exchanger designed for this application. Only a small sample of the total exhaust gas flow was used to evaluate catalysts B and C. The majority of the exhaust flow from the 5.7 l engine was bypassed around the catalyst core test piece. The flow of engine exhaust gas passing through the catalyst core was maintained at a space velocity of 60 000 $h^{-1}$ using an exhaust gas sampling pump.

## 3. Results and discussion

### 3.1. Preparation of metal-complex impregnated molecular sieves and the catalyst

The steps involved in the formation of catalysts are shown in the following scheme. The first step is to obtain an ion exchanged molecular sieve which is reacted with a ligand in the second step. Further palladium incorporation of the metal-complex impregnated molecular sieves in the third step results in the desired catalysts.

*Scheme*:

$$\mathrm{Cu(I)} + \text{MCM-41} \rightarrow \text{Cu-MCM-41} \xrightarrow{\mathrm{L1}} \text{L1Cu-MCM-41} \xrightarrow{\mathrm{Pd^{2+}}} \text{Catalyst A}$$

$$\mathrm{Cu(I)} + \text{MCM-41} \rightarrow \text{Cu-MCM-41} \xrightarrow{\mathrm{L2}} \text{L2Cu-MCM-41} \xrightarrow{\mathrm{Pd^{2+}}} \text{Catalyst B}$$

$$\mathrm{Fe(II)} + \text{MCM-41} \rightarrow \text{Cu-MCM-41} \xrightarrow{\mathrm{L2}} \text{L2Fe-MCM-41} \xrightarrow{\mathrm{Pd^{2+}}} \text{Catalyst C}$$

Molecular sieve (MCM-41) with a pore size of approximately 35 Å was used for this study. Iron(II) and copper(I) exchanged molecular sieves were obtained in a neutral solution. The XRD traces of Cu(I) and Fe(II) exchanged mesoporous molecular sieves are very similar to the untreated molecular sieves. There is only one peak in these traces in the range of $2\theta$=2–3°C. There are no additional peaks at $2\theta$=3–5°C, which suggest that the structure of the resultant MCM-41 does not have a perfect hexagonal arrangement. A disturbance in the hexagonal arrangement has been found responsible for the disappearance of those peaks.

The ion exchanged molecular sieves were reacted with solutions of the ligands prepared in situ. Condensation reactions of a primary amine with different aldehydes produce ligands L1 and L2 with the elimination of water. These ligands diffuse into the pores of the molecular sieves to produce complexes inside the pores. The Cu(I)–L2 and Fe(II)–L2 impregnated molecular sieves were studied by powder XRD. There was no change in both the XRD traces as compared with the Cu(I) and Fe(II) exchanged MCM-41. Such a retention of XRD peaks indicates complex formation in the pores of the molecular sieves and not on the surface. It is estimated that the linear dimensions of these ligands are approximately 20, whereas, the pore sizes of the molecular sieves are greater than 30. Thus the formation of these complexes in the pores of the molecular sieves (MCM-41) are not sterically constrained. Our attempts to synthesize these complexes in zeolite X and Y were unsuccessful.

During our complex forming reactions, a sharp color change was observed, which is indicative of the formation of metal complexes. These colors originate from d–d or ligand-to-metal charge transfer transitions. For example, colorless Cu(I) exchanged molecular sieve reacts with L1 to produce a bright yellow solid. The diffused reflectance UV–vis spectrum of this modified molecular sieve exhibits a peak around 370 nm, which is proposed to be a charge transfer transition. The peak in the diffused reflectance UV–vis spectrum of [Cu(I)]–L2 impregnated molecular sieve is shifted to a higher wavelength, due to lower ligand field splitting. Similar behaviors are observed for $[Cu(I)_2L1]^{2+}$ and $[Cu(I)_2L2]^{2+}$ complexes in solution [10]. Different ligands provide different electronic environments for the same metal ion which are manifested in different reactivity and catalytic properties. Not only the electronic nature of ligands, the coordination number of metal ions also have a profound impact on complex formation. The coordination number for metal ions are generally satisfied by the ligands, except in one case. Ligand L1 provides four coordination sites per ion. Due to the rigid structure of the ligand, the nitrogen atoms on one side of the benzene ring cannot come close to the nitrogen atoms on the other side of the ring. Since iron(II) prefers an octahedral coordination, and L1 cannot provide six coordination sites, there is no indication of a Fe(II)–L1 complex formation inside the molecular sieve pore.

The impregnation of copper and iron complexes inside the molecular sieve pores was further studied by FTIR spectroscopy. The copper ion exchanged molecular sieve has IR peaks at ~3500 (vs,br), 1640 (s), 1100 (vs,br) and 800 (vs) $cm^{-1}$. Upon complexation with the ligand L2, there was an additional peak at 1540 $cm^{-1}$. The peak at 1540 $cm^{-1}$ is very characteristic of metal-complexes with pyridine ligands. The IR spectrum of Fe(II)-exchanged molecular sieves is dominated by peaks at 1230 (vs,br), 1070 (vs,br) and 800 (s) $cm^{-1}$. The iron complex exchanged molecular sieve has additional IR peaks at ~2970 (w), 1635 (m), 1575 (w), 1450 (m), and 1360 (w) $cm^{-1}$. These peaks are characteristic of metal-complexes with pyridine ligands and thus suggests the formation of metal complexes inside zeolite pores [11] .

Finally, stirring and/or refluxing the metal-complex impregnated molecular sieves with $[Pd(NH_3)_4]Cl_2$ in DMF, resulted in the partial impregnation of $[Pd(NH_3)_4]^{2+}$ in MCM-41. Soxhlet extraction of the soluble impurities with acetonitrile produces catalysts A and B which contain copper(I) complexes, and catalyst C which contains an iron(II) complex. The impregnation of $Pd(NH_3)_4^{2+}$ in catalyst C was indicated by the appearance of additional IR peaks at 3540 (w) and 3270 (m) $cm^{-1}$ [11]. The XRD traces of catalysts B and C show broad peaks at $2\theta=41$ and 47 which could be attributed to $Pd(NH_3)_4Cl$. There is a possibility that some of the Pd(II) species are adsorbed on the surface of the molecular sieves. Elemental analysis has helped us to obtain the ratios of different elements in catalyst B. The elemental ratios are, Si/Al=14.7, Al/Cu=2.3, Al/Pd=3.7, Cu/Pd=1.5, C/Cu=27.8, and N/Cu=10.58. The empirical formula of catalyst B is $Na_{0.1}Pd_{0.6}CuL2Al_{2.3}Si_{34}O_y{\cdot}zH_2O$. Similarly, elemental ratios from catalyst C are Si/Al=13, Al/Fe=3.6, Al/Pd=5, Fe/Pd=1.3, C/Fe=21, N/Fe=8. The empirical formula for the iron complex impregnated molecular sieves is $Na_{0.6}Fe_3L2_2Pd_{2.2}Al_{11}Si_{143}O_y{\cdot}zH_2O$.

### 3.2. *Catalytic activity with simulated exhaust gas*

A mixture of 2% $^{15}NO$ and 2% $^{13}CO$ in argon, and 2% $H_2O$ and 2% $O_2$ in helium was used as a simulated exhaust gas. The gas mixture was introduced into the sample chamber under vacuum and allowed to interact with catalysts A, B and C. During the interaction of the source gas with the catalysts, the resulting gas was analyzed by the QMS. By using isotopically labeled gases, the reactants and products (nitrogen and carbon dioxide) could be positively identified due to their unique molecular mass as shown by the following equations:

Table 2
Mass spectroscopic intensities of $^{15}NO$ and $^{15}N_2$

| Sample | Temp. (°C) | $m/z$ 30 Abs. int.[a] (conc. of $^{15}N_2$) | $m/z$ 31 Intensity (conc. of $^{15}NO$) | Conversion (%) ($^{15}N_2/^{15}NO$) |
|---|---|---|---|---|
| Catalyst A | 100 | 2.61E−10 | 7.94E−09 | 3.29 |
| | 200 | 3.41E−10 | 6.88E−09 | 4.96 |
| Catalyst B | 100 | 9.80E−11 | 1.10E−09 | 8.90 |
| | 200 | 1.08E−10 | 5.60E−10 | 19.28 |
| Desorption | 211 | 6.45E−10 | 2.40E−10 | 272.5 |
| | 220 | 1.24E−09 | 4.57E−10 | 270.5 |
| | 226 | 1.63E−09 | 5.63E−10 | 288.9 |
| | 245 | 2.99E−09 | 6.50E−10 | 459.7 |
| Catalyst C | 100 | 1.67E−10 | 1.91E−09 | 8.75 |
| | 200 | 2.53E−10 | 3.30E−09 | 7.68 |

[a] Abs int. is calculated by subtracting background intensity from the leak intensity.

$$^{15}\mathrm{NO}\ (m/z = 31) \rightarrow {}^{15}\ \mathrm{N}_2\ (m/z = 30) \tag{3}$$

$$^{13}\mathrm{CO}\ (m/z = 29) \rightarrow {}^{13}\ \mathrm{CO}_2\ (m/z = 45) \tag{4}$$

The activity of catalysts A, B and C was investigated at different temperatures. The intensity of $^{15}NO$ and $^{15}N_2$ obtained from the analog mass spectroscopic scans are listed in Table 2. It is clear that substantial conversion of NO to $N_2$ was realized by our catalyst. We also observed a considerable increase in intensity of the peak at $m/z$=45, which is attributed to the formation of $^{13}CO_2$. In our experiments, we did not observe the formation of $^{15}N_2O$. The absence of a peak at $m/z$=46 indicates that nitrous oxide did not form during the catalytic reaction.

From data listed in Table 2, it is clear that the materials tested here show varying activity towards the reduction of nitric oxide to nitrogen. While catalyst B presents a conversion ratio over 19.28%, considerably lower activity is observed for catalysts A and C. It is interesting to note the difference in reactivity with the change in ligand and the metal ion. Although we have not measured the redox potentials of Cu–L1 and Cu–L2 in solution, we have observed that Cu–L2 is a better reducing agent. Many Cu(I) complexes with pyridine are strongly reducing. The reducing property seems to be maintained in the molecular sieve pores and is observed for the reduction of NO. Although catalysts B and C have the same ligand, the metal ions are different. The difference is manifested in the $NO_x$ reduction capability. In the reported literature, copper ion exchanged zeolites are better selective $NO_x$ reduction catalysts (SCR) as compared to the iron exchanged zeolite.

We also performed desorption studies on catalyst B by cutting off the source gas and heating the catalyst at higher temperatures. As observed in Table 2, a huge quantity of nitrogen is given off, which was adsorbed on the catalyst surface after $NO_x$ reduction at lower temperatures. An equal amount of carbon dioxide was also liberated. The experiments were not detailed enough to conclude that the reaction rates are desorption limited below 210°C. However, different adsorption and desorption situations may exist below 210°C: (a) considerable amounts of reactants are adsorbed below 210°C which are converted to products (nitrogen and carbon dioxide) only at higher temperatures and the products are desorbed quickly, and (b) considerable amounts of products are formed which are adsorbed below 210°C. These are only desorbed at higher temperatures. It is also difficult to calculate a catalytic turnover number from such an experiment, but we can conclude that the system is catalytic. We also concluded that the catalyst should be operated at approximately 250°C for better performance.

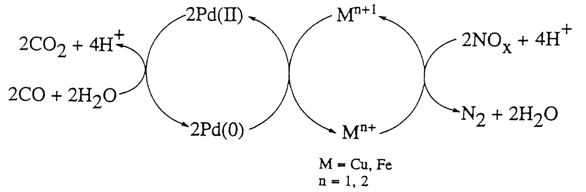

Fig. 3. The proposed catalytic cycle.

We have used a unique concept of incorporating two different types of metal ions in the pores of a molecular sieve. Two separate reactions take place at these metal centers. A reduction of $NO_x$ takes place on the iron or copper center of the respective metal complex, whereas an oxidation of carbon monoxide is assisted by the palladium ion. The oxidation and the reduction steps are coupled inside the molecular sieve pores which enable the catalytic process. While several mechanisms are possible, a conceptual catalytic cycle is depicted in Fig. 3. While no detailed mechanistic work was performed, the proposed mechanism is based on the literature and empirical observations. Palladium(II) ions are known to react with carbon monoxide and water to produce carbon dioxide. When water was not present in our simulated exhaust mixture, we did not see any carbon dioxide and the $NO_x$ conversion was very low. This might suggest that not only palladium(II) in the molecular sieves is active in CO oxidation, it also activates the other metal ion. Copper and iron complexes in solution are known to reduce nitrogen oxides [15]. While more controlled in the solution state, some of these reactions are also possible in the solid state. A complex impregnated molecular sieve is proposed to retain similar reactivity. In such reactions, the metal ions convert to higher oxidation state. Intra-zeolitic electron transfer is a known phenomenon, and our catalyst synthesis takes advantage of that phenomenon to regenerate the active states of palladium and the base metals (iron and copper).

### 3.3. *Catalytic activity with engine exhaust gas*

Catalyst efficiency tests were sequentially performed starting from low temperatures and then proceeding to higher temperatures, as described earlier. The conversion of HC, CO, and $NO_x$ catalyst B was only evaluated at a HC/$NO_x$ ratio of 2:1 which is shown in Fig. 4. Catalytic conversions of HC, CO, and $NO_x$ by catalyst C were obtained under two exhaust conditions. The catalytic conversion under higher hydrocarbon exhaust conditions (HC/$NO_x$=2.0/1.0) is shown in Fig. 5. The catalytic conversion of HC, CO, and $NO_x$ in an exhaust gas hydrocarbon concentration of 825 ppmC (HC/$NO_x$=0.42/1.0) is shown in Fig. 6.

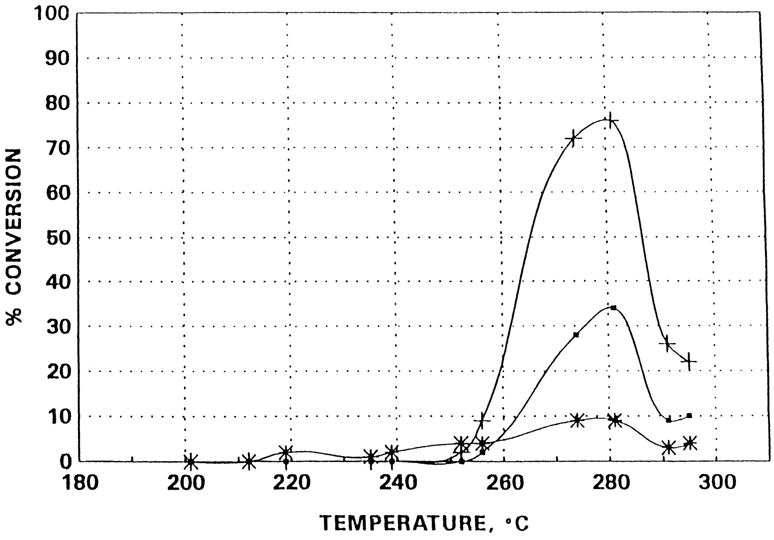

Fig. 4. Light-off temperature test for catalyst B under HC/$NO_x$=2.0/1.0 in the engine exhaust. HC (■), CO (+) and $NO_x$ (*).

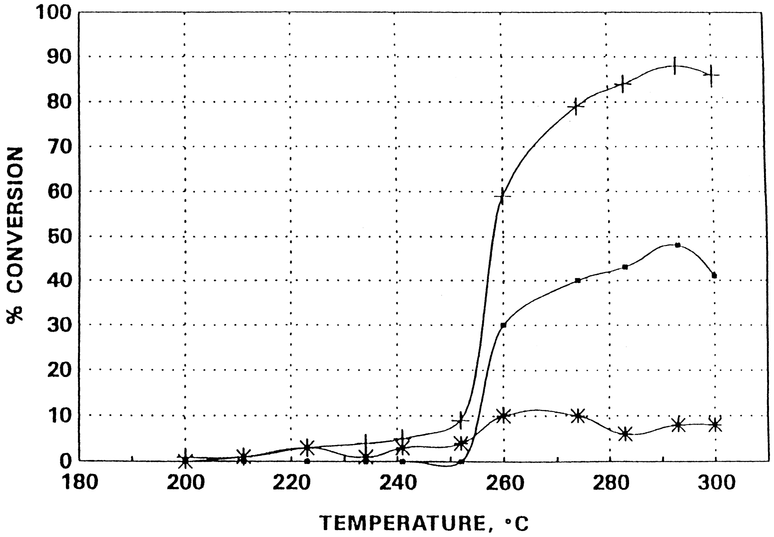

Fig. 5. Light-off temperature test for catalyst C under HC/$NO_x$=2.0/1.0 in the engine exhaust. HC (■), CO (+) and $NO_x$ (*).

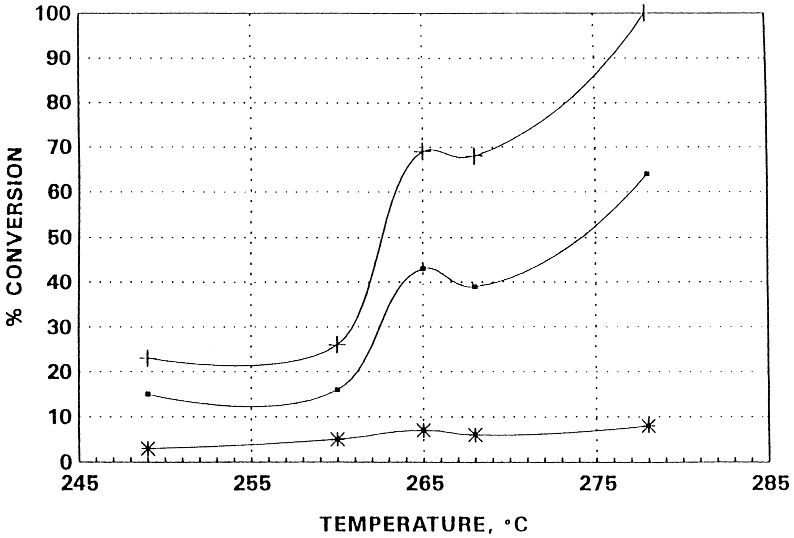

Fig. 6. Light-off temperature test for catalyst C under HC/$NO_x$=0.42/1.0 in the engine exhaust. HC (■), CO (+) and $NO_x$ (*).

With the 4000 ppmC hydrocarbon concentration in the exhaust (HC/$NO_x$=2.0/1.0, Fig. 4), catalyst B is active in a narrow temperature range of 270–285°C, with maximum activity at 280°C. At that temperature, conversion of CO, HC and $NO_x$ are 76%, 34% and 10%, respectively. Maximum oxidation efficiencies of catalyst C for HC and CO were obtained (Fig. 5) at a temperature of 293°C and were found to be 48% and 88%, respectively. In the temperature range from 260°C to 280°C, a 10% reduction of $NO_x$ was observed. In a relatively low HC-to-$NO_x$ ratio environment (HC/$NO_x$=0.42/1.0), a maximum of 8% $NO_x$ reduction was observed with catalyst C (Fig. 6). Most of the other experimental lean-$NO_x$ catalysts [12–14] are inactive under such conditions. Carbon monoxide was almost completely oxidized at a temperature of

278°C. A 64% removal of hydrocarbon was observed during this experiment. Our preliminary durability studies were performed at 270°C for 8 h. The studies suggest inappreciable change in activity for $NO_x$ reduction over time.

Although, the composition of the engine exhaust gas is much more complex as compared to the simulated exhaust gas, our unique concept of coupling the oxidation and reduction cycles is still operative. However, we have been disappointed by the activity of catalyst B which showed a substantial conversion under simulated exhaust conditions. Copper(I)-based, catalyst B might be more susceptible to poisoning than iron(II) based catalyst. The following reactions (Eqs. (5)–(10)) are probable during the catalytic process if the engine exhaust is simply treated as a mixture of HC, CO, $NO_x$, $O_2$ and $H_2O$. Although we have not proved the detail reaction mechanism for $NO_x$ catalysis, the above reactions could elucidate the observed reactivity patterns. The interactions of $NO_x$ and $O_2$ with the iron and copper complexes are competitive. Increased reactivity of $NO_x$ as compared to $O_2$ can be obtained either by changing the metal ion or the ligand. This leads us to believe that a metal complex is critical for our catalyst.

$$2\mathrm{M}^{n+} + 2\mathrm{NO} \rightarrow \mathrm{M}_2^{n+1}(\mathrm{N_2O_2^{2-}}) \tag{5}$$

$$\begin{aligned} &2\mathrm{M}^{n+} + (\mathrm{N}_2 O_2^{2-}) + 2\mathrm{M}^{n+} + 4\mathrm{H}^+ \\ &\quad \rightarrow 4\mathrm{M}^{n+1} + \mathrm{N}_2 + 2\mathrm{H_2O} \end{aligned} \tag{6}$$

$$2\mathrm{M}^{n+} + \mathrm{O}_2 \rightarrow \mathrm{M}_2^{n+1}(\mathrm{O_2^{2-}}) \tag{7}$$

$$\mathrm{M}_2^{n+1}(\mathrm{O_2^{2-}}) + \mathrm{HC} \rightarrow \mathrm{Oxidized\,HC} + 2\mathrm{M}^{n+1} \tag{8}$$

$$2\mathrm{Pd(II)} + 2\mathrm{CO} + 2\mathrm{H_2O} \rightarrow 2\mathrm{Pd(0)} + 2\mathrm{CO_2} + 4\mathrm{H}^+ \tag{9}$$

$$4\mathrm{M}^{n+1} + 2\mathrm{Pd(0)} \rightarrow 4\mathrm{M}^{n+} + 2\mathrm{Pd(II)} \tag{10}$$

Our work clearly shows that metal-complex impregnated molecular sieves are capable of catalyzing $NO_x$ reductions. When a second metal ion such as Pd(II) is incorporated, it carries out an overall reaction as shown in Eq. (11). Such a reaction bypasses the necessity of additional reducing gases such as hydrocarbons and can be conveniently used to obtain lean-$NO_x$ reduction. Such a reaction is not catalyzed by a simple ion exchanged zeolite.

$$2\mathrm{NO} + 2\mathrm{CO} \rightarrow \mathrm{N}_2 + 2\mathrm{CO}_2 \tag{11}$$

Our catalyst is active at a temperature range of 260–285°C which is significantly different from the operating temperatures of the platinum and copper exchanged zeolites. The platinum exchanged zeolite is active at nearly 200°C, whereas the copper exchanged zeolite is active around 325°C.

## 4. Conclusion

Lean-$NO_x$ catalysts have been developed which operate under an oxygen-rich exhaust environment and do not need a reducing gas such as hydrocarbon. The catalysts operate in a temperature range of 260–285°C which make these viable for the control of $NO_x$ in relatively cool exhaust gas, such as from diesel engines. We do not believe that the ligand used in this study is stable at high temperatures, thus limiting the catalyst's use to only colder emission. Metal complexes of highly conjugated planar ligands are stable to very high temperatures. The choice of a suitable ligand might enable us to treat exhaust at higher temperatures. Our catalysts are based on copper and iron which are less expensive as compared to the noble metal containing catalyst. The lean-$NO_x$ catalyst technology is largely experimental at present. Studies conducted on the lean $NO_x$ catalytic converter technology on a heavy duty diesel engine [14] show a maximum $NO_x$ reduction of 30–40% only in the presence of huge quantities of supplemental hydrocarbon (HC/$NO_x$ ratio nearly 10.0/1.0). A high hydrocarbon requirement for the catalytic $NO_x$ conversion defeats the efficiency and fuel economy of an automobile. Though our catalysts at present only achieve a 10% $NO_x$ reduction, our catalysts operate under a very low hydrocarbon concentration under which other experimental catalysts show no activity. We believe that additional research and development will result in a superior lean-$NO_x$ catalyst.

## Acknowledgements

This work was supported by Southwest Research Institute (SwRI) under the Internal Research and Development (IR&D) Program. Technical help of Mr. Walter Machowski, Mr. Stephen Salazar, Mr. Tom Gabehart and Mr. Brian Haby is greatly appreciated.

## References

[1] Applied for US patent.

[2] National Air Quality and Emission Trends Report, 1992, US EPA, Research Triangle Park, NC, October 1993.

[3] B.C. Berks, S.J. Fergusan, J.W.B. Moir, D.J. Richardson, Biochim. Biophys. Acta 1232 (1995) 97–173.

[4] L.I. Hochstein, G.A. Tomlinson, Ann. Rev. Microbiol. 42 (1988) 231–261 and references cited therein; R. Knowles, Microbiol. Rev. 46 (1982) 43.

[5] J. Reedijk, Bioinorganic Catalysis, Marcel Dekker, New York, 1993 and references therein.

[6] P.P. Paul, M.A. Miller, M.J. Heimrich, S.T. Schwab, Proc. Mater. Res. Soc. 431 (1996) 117–121.

[7] D.F. Shriver, M.A. Drezdzon, The Manipulation of Air-Sensitive Compounds, Wiley, New York, 1986 and references therein.

[8] J.S. Beck, C.T. Chu, I.D. Johnson, C.T. Kresge, M.E. Leonowicz, W.J. Roth, J.C. Vartuli, WO Patent 91/11390.

[9] N. Herron, J. Coord. Chem. 19 (1988) 25–38.

[10] J. Jazwinski, J.M. Lehn, D. Lilenbaum, R. Ziessel, J. Guilhem, C. Pascard, J. Chem. Soc., Chem. Commun. (1987) 1691.

[11] C.J. Pouchart, The Aldrich Library of Infrared Spectra, 3rd ed., Aldrich Chemical Company, Milwaukee, WI, 1981.

[12] B.H. Engler, J. Leyrer, E.S. Lox, K. Ostgathe, SAE Paper 930735, Detroit, Michigan, 1–5 March, 1993.

[13] M.J. Heimrich, M.L. Deviney, SAE Paper 930 736, Detroit, MI, 1–5 March, 1993.

[14] M.J. Heimrich, Final Report for the California Air Resources Board, ARB Contract No. 92-310, May, 1996.

[15] P.P. Paul, K.D. Karlin, J. Am. Chem. Soc. 113 (1991) 6331.